nature nanotechnology

LETTERS

PUBLISHED ONLINE: 3 FEBRUARY 2013 | DOI: 10.1038/NNANO.2012.263

Direct detection of a *BRAF* mutation in total RNA from melanoma cells using cantilever arrays

F. Huber[1]*, H. P. Lang[1], N. Backmann[1], D. Rimoldi[2†] and Ch. Gerber[1†]

Malignant melanoma, the deadliest form of skin cancer, is characterized by a predominant mutation in the *BRAF* gene[1–3]. Drugs that target tumours carrying this mutation have recently entered the clinic[4–7]. Accordingly, patients are routinely screened for mutations in this gene to determine whether they can benefit from this type of treatment. The current gold standard for mutation screening uses real-time polymerase chain reaction and sequencing methods[8]. Here we show that an assay based on microcantilever arrays can detect the mutation nanomechanically without amplification in total RNA samples isolated from melanoma cells. The assay is based on a *BRAF*-specific oligonucleotide probe. We detected mutant *BRAF* at a concentration of 500 pM in a 50-fold excess of the wild-type sequence. The method was able to distinguish melanoma cells carrying the mutation from wild-type cells using as little as 20 ng μl^{-1} of RNA material, without prior PCR amplification and use of labels.

In the past decade, the identification of alterations in specific signalling pathways and recurrent oncogenic mutations in particular types of cancers has led to the explosion of targeted therapy approaches. In cutaneous melanoma, a significant improvement in overall survival has been achieved by the use of vemurafenib and similar drugs that selectively inhibit tumours carrying a mutated *BRAF* gene[4,5]. Further drugs for combination therapies with higher efficacies and fewer side effects are in clinical trials[6]. *BRAF* is one of three *RAF* genes (rapidly accelerated fibrosarcoma A, B and C) encoding cytoplasmic protein serine/threonine kinases belonging to the mitogen-activated protein kinase (MAPK) signal transduction cascade, a pathway controlling various cellular processes such as proliferation, migration and survival[1,7]. *BRAF* somatic mutations are present in half of cutaneous melanomas. Over 90% of the mutations are a single T to A transversion at position 1799 in the BRAF coding sequence (cT1799A), which converts a valine amino-acid residue at position 600 in the protein to a glutamic acid (V600E). This mutation renders the protein constitutively active, resulting in a deregulated MAPK pathway[2] and thus uncontrolled cell growth and cancer. *BRAF* mutations are also present in other neoplasms, including hairy cell leukaemias, and thyroid and colon carcinomas[3,9,10]. As the presence of the cT1799A/V600E *BRAF* (hereafter $BRAF^{V600E}$) mutation determines eligibility for BRAF inhibitor treatment, molecular screening of tumour biopsies is now carried out routinely. Various methods have been developed for the detection of the $BRAF^{V600E}$ mutation at the DNA level. Among them is the long-established procedure of polymerase chain reaction (PCR) amplification coupled with Sanger sequencing of the product. The standard test currently used to analyse patients' biopsies before initiation of vemurafenib treatment relies on real-time PCR (the COBAS Test[8]), whereby 5–10% of *BRAF*-mutated melanoma cells can be detected in a background of normal cells. Alternative technologies to classic methods are under development, such as cycling temperature capillary electrophoresis[11] (with sensitivity comparable to COBAS), silicon nanowire field-effect transistors[12] and a three-dimensional gold nanowire platform[13]. The latter technologies have only been shown to work using synthetic oligonucleotide targets or larger gene fragments, or indeed still rely on an initial PCR amplification. In particular, they have not been applied to the direct identification of a mutated messenger RNA (mRNA) sequence in total RNA (constituted primarily by ribosomal RNA and containing all mRNAs transcribed from genes) or DNA samples.

In recent years, a versatile platform for biodetection has been developed based on microfabricated arrays of silicon cantilevers[14–21], each coated with a sensitive layer for molecular recognition, for example, a gene-specific oligonucleotide. The binding of the target sequence is mechanically transduced to the cantilever surface, resulting in bending of the cantilever. Such devices comprise ultrasensitive sensors for the detection of biochemical interactions in liquid environments[22]. Here we have explored the feasibility of applying this technology to discriminate between $BRAF^{V600E}$ and wild-type *BRAF* sequences in melanoma samples.

In a first set of experiments aimed at assessing the specificity of detection of the $BRAF^{V600E}$ mutation with cantilever arrays, we chose as a probe a surface-immobilized thiolated 13-mer oligonucleotide (V600E_short; Table 1) carrying at its centre the mutated nucleotide (adenine instead of thymidine, labelled in red). The short length is sufficient to provide a unique sequence that is not present anywhere else in the *BRAF* PCR product, and a central position of the mismatch was selected as it allows the highest discrimination between the wild-type and the mutant sequence. To ensure a high surface density of the *BRAF*-specific probe layer, preliminary tests were performed to optimize the adsorption of V600E_short thiol oligonucleotide probes onto a gold-coated cantilever surface (Supplementary Figs S1 and S2). Based on the results obtained, we decided to use the highest concentration (40 μM), corresponding to over 90% occupancy[23], thus ensuring a large cantilever bending signal in all subsequent hybridization experiments. We also confirmed the reusability of the sensor by repeated injections of a 13-mer complementary oligonucleotide preceded by urea washing steps (Supplementary Fig. S3).

We applied the array functionalized as shown in Fig. 1 to distinguish between wild-type and mutated *BRAF* sequences. For these experiments, we used PCR-amplified cDNA (complementary DNA derived from mRNA by reverse transcription) samples ($BRAF^{V600E}$ PCR, 621 base pairs (bp) long) derived from melanoma cells expressing either wild-type *BRAF* or mutant $BRAF^{V600E}$. Figure 2a shows the differential signals obtained after injection of pure wild-type or mutated *BRAF* sequences, as well as after injection of increasing dilutions (wild type-to-mutant ratios from 1:1 to 50:1) of the mutated into the wild-type sequence.

[1]Swiss Nano Institute, University of Basel, Klingelbergstrasse 82, 4056 Basel, Switzerland, [2]Ludwig Center for Cancer Research of the University of Lausanne, 1066 Epalinges, Switzerland; †These authors contributed equally to this work. *e-mail: francois.huber@unibas.ch

Table 1 | Oligonucleotide probes used in the study.

Probe	Sequence	Use
V600E_short	5′-CTACAG**A**GAAATC-3′	Detection of 621 bp mutated cDNA PCR product (Fig. 2)
polyAC_short	5′-ACACACACACACA-3′	Reference for detection of 621 bp mutated cDNA PCR product (Fig. 2)
V600E_long	5′-GAGATTTC**T**CTGTAGCTA-3′	Detection of *BRAF*^{V600E} in total RNA (Figs 3 and 4)
polyAC_long	5′-ACACACACACACACACAC-3′	Reference for *BRAF* RNA detection (Figs 3 and 4)
wt_long	5′-GAGATTTC**A**CTGTAGCTA-3′	Additional reference in *BRAF*^{V600E} detection (Fig. 3e,f)

The nucleotides important for detection (corresponding to the cT1799A/V600E mutation) are labelled in red. Note that V600E short and long, both designed to detect the mutation, were chosen from opposite DNA strands (hence the different, but complementary, sequence).

The cantilevers selectively responded to the mutated *BRAF* sequence, and the amplitude of deflection scaled with the concentration of target DNA or RNA. Furthermore, the mutant gene sequence could still be detected in the presence of a 50-fold excess of wild-type DNA sample (that is, when present at the 2% level). In each experiment the total DNA concentration was kept constant at 10 ng μl^{-1}. As the size of the fragments used was 621 bp, corresponding to a molecular weight of 4×10^5 Da, the results indicate a detection limit of ~500 pM *BRAF*^{V600E} DNA in the presence of excess wild-type sequence. Figure 2b shows the Langmuir isotherm fitted to the equilibrium values of responses extracted from Fig. 2a, plotted against the concentration of *BRAF*^{V600E} PCR product. The dG value of -49.8 kJ mol^{-1} calculated from the Langmuir plot is in good agreement with results previously reported for hybridization experiments with oligonucleotides of similar length using microcantilevers (d$G = -41.4$ kJ mol^{-1})[15] and surface plasmon resonance (SPR) data (d$G = -43.4$ kJ mol^{-1})[24], as well as theoretical calculations in solution (d$G = -50.5$ kJ mol^{-1})[25]. The minor deviation of our measurement from these values can be explained by the double-stranded nature and length of the fragments analysed.

Messenger RNAs are present in cells at a higher copy number than the corresponding genes. In addition, RNA/DNA interactions are stronger than DNA/DNA interactions[26]. We thus directly detected the *BRAF* mutation at the RNA level without prior amplification steps (for example, PCR). For this purpose we designed an oligonucleotide probe to unambiguously identify the mutated *BRAF*

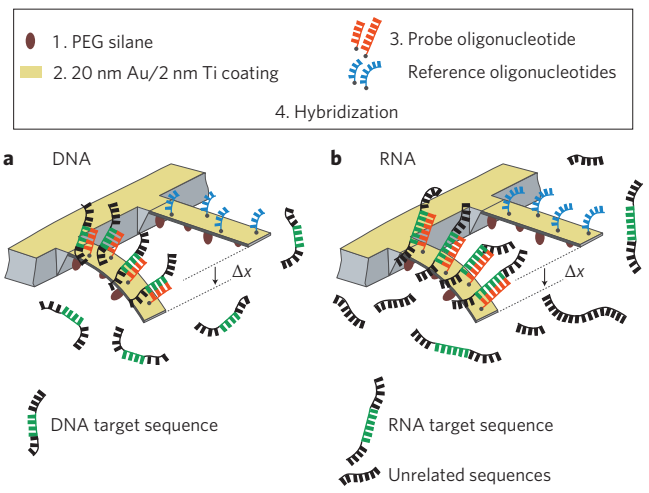

Figure 1 | Principle of microcantilever array functionalization and measurement. a,**b**, Steps: (1) the silicon array is coated with PEG–silane (brown ovals) to prevent non-specific adsorption to the lower cantilever side; (2) the array is coated with titanium as an adhesion layer and gold (in yellow) for thiol binding; (3) the cantilevers are either functionalized with a probe oligonucleotide (in red) or a non-specific reference oligonucleotide (in light blue); (4) injection of the target DNA (**a**) or RNA (**b**) containing the complementary (matching) sequence (depicted in green) to the probe oligonucleotide (red). Non-related sequences are shown in black. On hybridization, only the probe cantilever bends, giving rise to a differential deflection Δx. No binding occurs on the reference cantilever.

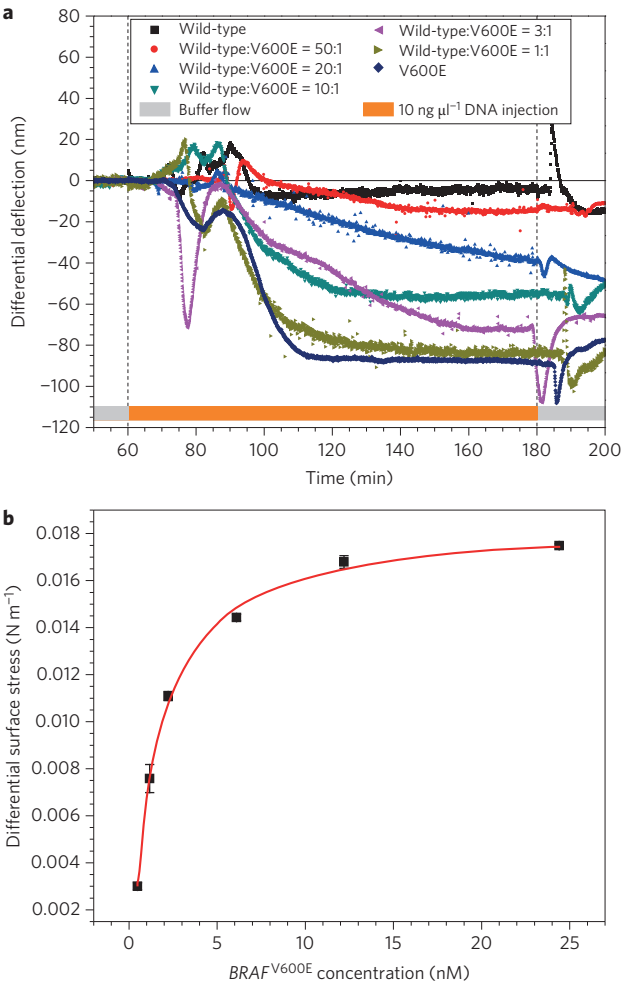

Figure 2 | Compressive surface stress from hybridization experiments with PCR-amplified *BRAF* sequences. a, Differential surface stress measured after injection of different ratios of wild-type to mutant DNA, as indicated. Differential signals between probe (derivatized with V600E_short) and reference (derivatized with polyAC_short) cantilevers are shown. Fluctuations after sample injection are due to mixing of buffer, DNA solution and switching of valves, but do not influence the later equilibrium cantilever deflection before performing a washing step with 5× SSC. The differently coloured bars at the bottom indicate the duration of injection and the solution being injected (light grey, buffer; orange, DNA sample). The dashed vertical lines separate different injections. **b**, Langmuir isotherm with $R^2 = 0.97$, indicating a reliable fit with the data. The experiments show that the 13-mer *BRAF* sequence can be detected in a larger DNA fragment at various concentrations.

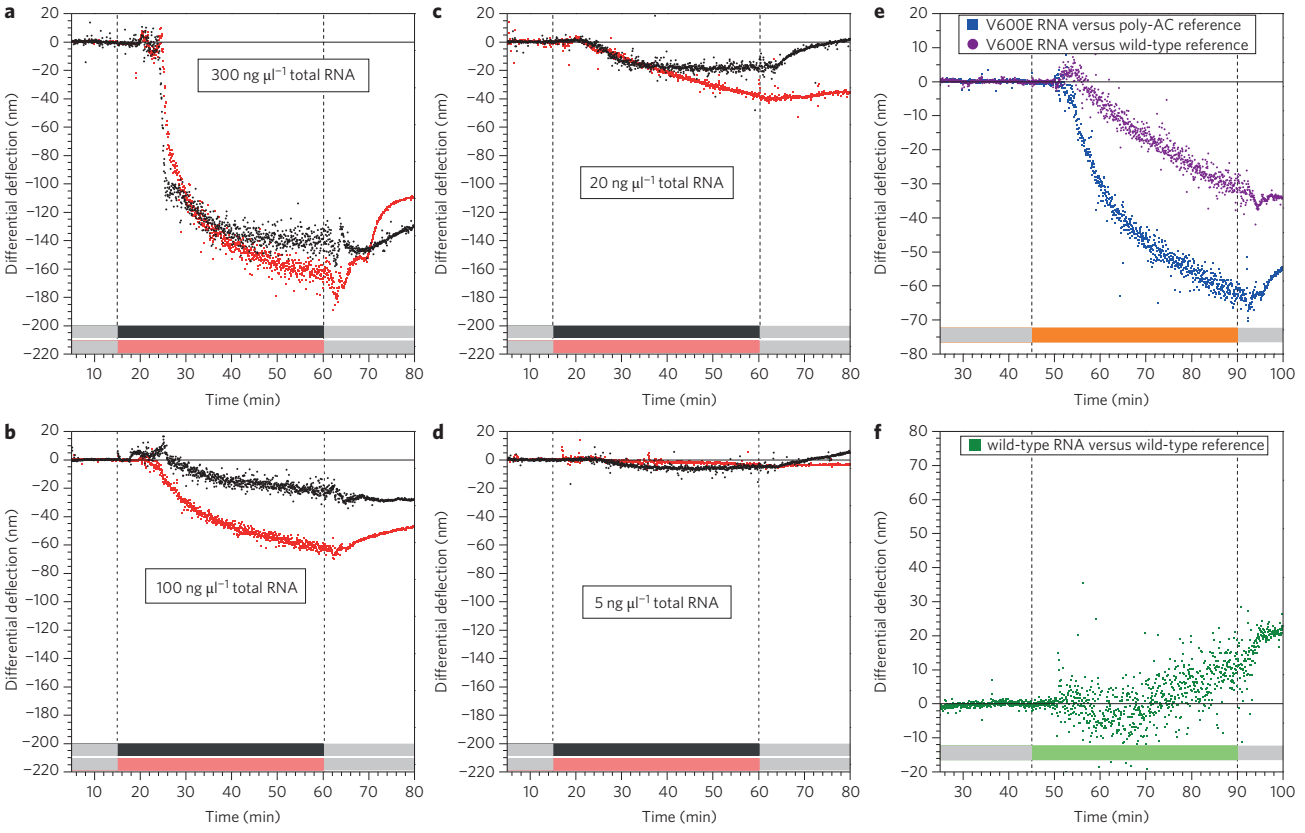

Figure 3 | Detection of mutated versus wild-type BRAF in total RNA samples. a–d, Total RNA samples from T618A (wild-type, black) and SK-Mel-37 (*BRAF*^{V600E}, red) cells were injected at the indicated concentrations. The bars at the bottom of the graphs indicate the solution being injected, and different injection periods are marked by dashed vertical lines: buffer (light grey), total RNA from T618A (dark grey) and SK-Mel-37 (light red) cell lines. Differential signals between probe (V600E_long functionalized) and reference (polyAC_long functionalized) cantilevers are shown. At the highest concentration measured (300 ng µl^{-1}, **a**), mutant and wild-type sequences cannot be clearly distinguished, indicating increased cross-hybridization by the wild-type sequence. We are able to reliably distinguish mutant BRAF from wild-type BRAF at concentrations of 100 and 20 ng µl^{-1} (**b**,**c**). A signal of 4 nm at a total RNA concentration as low as 5 ng µl^{-1} was observed (**d**), indicating a limit of detection between 5 and 20 ng µl^{-1}. **e**, Experiments using total RNA from SK-Mel-37 cells and poly-AC (blue dots) or wild-type (purple dots) oligonucleotides as references, respectively (light grey bars indicate buffer and the orange bar indicates SK-Mel-37 sample injection). **f**, Response of total RNA to wild-type T618A (injection of sample indicated by light green bar at the bottom) is shown using a wild-type oligonucleotide reference (green dots). Here we show that the assay can distinguish between wild-type and mutant *BRAF* mRNA in a complex background of non-related sequences.

mRNA sequence. Based on the expressed sequence tags database of the human genome we determined a minimum required length of 18 bases to specifically detect *BRAF* mRNA. As total RNA is a more complex sample than uniform PCR products, longer oligonucleotide probes were chosen to avoid cross-reactivities and thus assure specificity. The cantilevers were therefore functionalized with the corresponding 18-mer thiol oligonucleotide probe (Table 1) and an 18-mer reference oligonucleotide (polyAC_long). The use of reference cantilevers is mandatory to eliminate temperature drift, unspecific binding and refractive index changes. Total RNA samples extracted from melanoma cell lines carrying wild-type (T618A) or mutated (SK-Mel-37) BRAF sequences were injected at different concentrations, ranging from 5 to 300 ng µl^{-1}. The results of these experiments are shown in Fig. 3a–d.

Four concentrations in the range 5–300 ng µl^{-1} were measured, suggesting a lower limit of detection between 5 and 20 ng µl^{-1} total RNA. Best specificities were achieved at 100 and 20 ng µl^{-1} total RNA (Fig. 3b,c). As *BRAF*-mutated cancer cells still retain a normal copy of the wild-type *BRAF* gene that can still be expressed, at variable levels, alongside the mutated form, using a wild-type *BRAF* oligonucleotide as a reference instead of polyAC_long provides an important control. Using the corresponding 18-mer wild-type oligonucleotide as reference, we observed a reduced response in the SK-Mel-37 signal (purple curve) compared to the poly-AC differential signal (blue curve, Fig. 3e), consistent with a certain level of wild-type *BRAF* expression in these cells (estimated at ~20% from Sanger sequencing plots, as shown in Supplementary Fig. S4). A positive signal (green curve) was observed using T618A RNA (*BRAF* wild-type), as expected, due to binding to the wild-type oligonucleotide (Fig. 3f). The increased noise observed during sample injection is probably due to the complexity of the total RNA samples. We further extended the RNA experiments to additional cell lines carrying either *BRAF*^{V600E} or wild-type *BRAF* sequences. Figure 4a,b shows the results of experiments performed by injecting total RNA (at a concentration of 100 ng µl^{-1}) extracted from three different mutant cell lines (SK-Mel-37, Me246.M1 and Me275) and two different wild-type cell lines (T618A and T1405B), respectively. The signals from the mutant cell lines differ substantially from those of the wild-type ones. The stronger deflection observed for SK-Mel-37 compared to the other two mutant cell lines correlates with the higher *BRAF* levels expressed by these cells (see Methods). The results demonstrate the robustness of the assay to readily distinguish *BRAF*-mutated from *BRAF* wild-type cell lines.

In summary, the experiments with melanoma samples demonstrate that mutant *BRAF*^{V600E} can be identified in PCR products

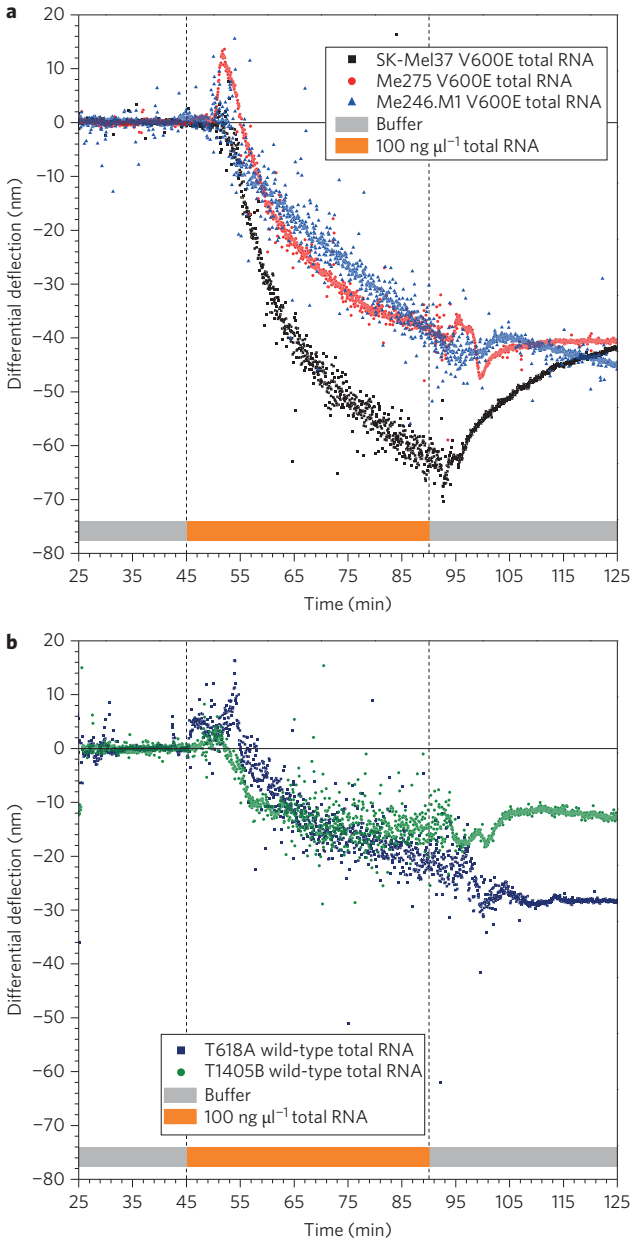

Figure 4 | Analysis of RNA samples from different *BRAF* mutated and wild-type tumour cells. Differential signals between probe (V600E_long functionalized) and reference (polyAC_long functionalized) cantilevers are shown. **a**,**b**, Total RNA from mutant $BRAF^{V600E}$ cell lines (**a**) consistently shows a higher signal than RNA from wild-type samples (**b**). After equilibrating the microcantilever array with 0.01× SSC buffer (light grey bar), 450 µl of total RNA (100 ng µl^{-1}) was injected (orange bar). Dashed vertical lines indicate different injection periods. This experiment shows that the assay does not depend on the cell lines used; different *BRAF* mutant cell lines can be distinguished from wild-type cell lines.

as well as in total RNA extracted from mutant cancer cell lines. The low concentration of total RNA required for the assay described here (20 ng µl^{-1}) indicates that this approach is applicable to clinical material. Accordingly, this methodology could simplify and speed up the identification of tumours, reducing time to treatment. Although we have focused here on the detection of $BRAF^{V600E}$ mutations in melanoma, the microcantilever approach can be extended to other relevant mutations recurring in other types of cancer (for example, mutations in *KIT*, a receptor tyrosine kinase gene, in gastrointestinal stromal tumours and in epidermal growth factor receptor mutations in lung cancer[27]). The proposed method has the following advantages: (i) samples do not have to be labelled or pre-amplified by PCR, as total RNA samples can be utilized; (ii) the technique is cost-efficient; (iii) because of the array format the analysis can be paralleled, so the presence of multiple mutations may be interrogated simultaneously, allowing a more detailed clinical prognosis, facilitating fast and personalized medical diagnostics.

Methods

Sensor preparation. Microcantilever arrays of eight silicon cantilevers (500 µm long, 100 µm wide and 1 µm thick), fabricated at IBM Research, were used in the experiments. To coat the microcantilever arrays with a receptor layer, we used a previously described procedure[28]. Briefly, the arrays were cleaned in Piranha solution (30% H_2O_2:96% H_2SO_4 = 1:1, vol/vol) for 15 min, rinsed three times with water followed by isopropanol, then dried in air. The arrays were then incubated for 30 min in 10 mM 2-[methoxypoly (ethyleneoxy)propyl] trimethoxysilane (7 ethylene glycol units, ABCR) solution in dry ethanol to reduce non-specific binding to the lower silicon side. The array was then rinsed with isopropanol and dried in air. The upper sides of the cantilevers were subsequently coated with a 2 nm layer of titanium followed by a 25 nm gold layer, without breaking the vacuum. Deposition of metal layers was performed in an EVA 300 electron beam evaporator (Alliance Concept) at an evaporation rate of 0.1 nm s^{-1}. Gold-coated arrays were used immediately.

Probes. Oligonucleotides functionalized at the 5′ end with a thiol group via a hexyl spacer were obtained from Microsynth. The synthetic oligonucleotides used in this work are described in Table 1. Oligonucleotides were dissolved in 50 mM triethyl ammonium acetate buffer (TEAA, Fluka), pH 7, at a concentration of 40 µM.

It is of paramount importance that measurements are performed in a differential fashion. External factors such as non-specific interactions and thermal drift are cancelled out by calculating the differential response of a probe and a reference cantilever (in this study derivatized with a non-specific oligonucleotide of the same length as the probe sequence or, in some experiments, with a wild-type sequence). Eight microcapillaries (outer diameter, 250 µm; inner diameter, 150 µm; King Precision Glass) were filled with the appropriate oligonucleotide solution (probe or reference) to functionalize the cantilevers either with a probe layer or a reference layer. The cantilever array was then washed in 0.01× sodium-buffered saline citrate (SSC, Fluka), 1.5 mM NaCl, and used directly for the analysis.

DNA and RNA sample preparation. Cell lines from melanoma metastases were established at LICR, except for SK-Mel-37 (a gift from Y.T. Chen, New York). SK-Mel-37, Me275 and Me246.M1 harbour mutated *BRAF* (cT1799A/V600E), while T618A and T1405B carry wild-type *BRAF*, as assessed by Sanger sequencing. Total BRAF mRNA expression relative to T618A (set at 1) was 1.2, 0.9, 2.5 and 0.7 for Me275, Me246.M1, SK-Mel-37 and T1405B, respectively, as estimated by RNAseq[29] and/or PCR. Wild-type or mutated *BRAF* DNA sequences (621 bp, spanning exon 13–18) were generated by PCR amplification of cDNA prepared from melanoma cell lines (T618Aand SK-Mel-37) as previously described[30]. Amplified products were concentrated by two rounds of ammonium acetate/ethanol precipitation and dissolved in TE buffer. Total RNA was extracted using Trizol reagent (Invitrogen) following the manufacturer's instructions. RNA was further purified by ammonium acetate/ethanol precipitation and dissolved in DEPC-treated H_2O.

Before the experiments, the PCR amplified fragments were denatured at 96 °C for 10 min and cooled in an ice bath, forming single-stranded segments along the DNA to enable hybridization. Similarly, total RNA was heated to 70 °C for 5 min and cooled, denaturing the three-dimensional structure of the RNA molecules to facilitate hybridization.

Sensor instrument. The functionalized array was inserted into a liquid chamber (volume, 15 µl), and cantilever bending was measured using time-multiplexed vertical-cavity surface-emitting lasers (VCSELs; wavelength 760 nm, Avalon Photonics). The laser beam was deflected to a position-sensitive detector (PSD, SiTek). Data were acquired using a multifunctional data-acquisition board (National Instruments) driven by LabView software. The software also controlled the liquid handling system of the setup, the syringe pump (GENIE, Kent Scientific) and a 10-position valve system (Rheodyne). The entire setup was placed inside a temperature-controlled box (Intertronic; Interdiscount), equilibrated through a fuzzy logic controller by the LabView software to keep the inside of the box at a temperature of 23 °C (accuracy of ± 0.02 °C).

Measurement and data analysis. Hybridization experiments for the PCR DNA fragments were conducted in 5× SSC, and total RNA hybridization was carried out in 0.01× SSC. A volume of 450 µl was injected at a continuous flow (rate, 5–10 µl min^{-1}). The bimetallic response and mechanical properties of the cantilevers were assessed by applying 0.3 V to a Peltier element situated directly below the chamber for 70 s (thermal cycle). This resulted in a 2 °C pulse for deflection calibration. The average of all cantilevers together with the largest

response was used to normalize the signal, provided that the deflections did not differ by more than 10% in magnitude (usually six or more cantilevers satisfy this criterion). The normalized data from the reference cantilevers were subtracted from the data for the probe cantilevers to obtain a differential signal. A baseline correction (required because the drift behaviour of the different cantilevers varies slightly) was applied, using a linear fit of the data in the time interval beginning with buffer injection followed by DNA or RNA samples, respectively. The slope of the linear fit was subtracted from all differential signals.

Received 15 October 2012; accepted 18 December 2012; published online 3 February 2013

References

1. Roskoski, R. RAF protein-serine/threonine kinases: structure and regulation. *Biochem. Biophys. Res. Commun.* **399,** 313–317 (2010).
2. Gray-Schopfer, V. C., da Rocha Dias, S. & Marais, R. The role of B-RAF in melanoma. *Cancer Metastasis Rev.* **24,** 165–183 (2005).
3. Davies, H. *et al.* Mutations of the *BRAF* gene in human cancer. *Nature* **417,** 949–954 (2002).
4. Ribas, A. & Flaherty, K. T. BRAF targeted therapy changes the treatment paradigm in melanoma. *Nature Rev. Clin. Oncol.* **8,** 426–433 (2011).
5. Flaherty, K. T. Dividing and conquering: controlling advanced melanoma by targeting oncogene-defined subsets. *Clin. Exp. Metastasis* **29,** 841–846 (2012).
6. Ravnan, M. C. & Matalka, M. S. Vemurafenib in patients with *BRAF V600E* mutation-positive advanced melanoma. *Clin. Ther.* **34,** 1474–1486 (2012).
7. Flaherty, K. T. *et al.* Improved survival with MEK inhibition in BRAF-mutated melanoma. *N. Engl. J. Med.* **367,** 107–114 (2012).
8. Halait, H. *et al.* Analytical performance of a real-time PCR-based assay for V600 mutations in the BRAF gene, used as the companion diagnostic test for the novel BRAF inhibitor Vemurafenib in metastatic melanoma. *Diagn. Mol. Pathol.* **21,** 1–8 (2012).
9. Pratilas, C. A., Xing, F. & Solit, D. B. Targeting oncogenic BRAF in human cancer. *Therapeut. Kinase Inhib.* **355,** 83–98 (2012).
10. Tiacci, E. *et al. BRAF* mutations in hairy-cell leukemia. *N. Engl. J. Med.* **364,** 2305–2315 (2011).
11. Hinselwood, D. C., Abrahamsen, T. W. & Ekstrøm, P. O. BRAF mutation detection and identification by cycling temperature capillary electrophoresis. *Electrophoresis* **26,** 2553–2561 (2005).
12. Wu, C. C. *et al.* Label-free biosensing of a gene mutation using a silicon nanowire field-effect transistor. *Biosens. Bioelectr.* **25,** 820–825 (2009).
13. Fang, Z. & Kelley, S. O. Direct electrocatalytic mRNA detection using PNA-nanowire sensors. *Anal. Chem.* **81,** 612–617 (2009).
14. Fritz, J. *et al.* Translating biomolecular recognition into nanomechanics. *Science* **288,** 316–318 (2000).
15. McKendry, R. *et al.* Multiple label-free biodetection and quantitative DNA-binding assays on a nanomechanical cantilever array. *Proc. Natl Acad. Sci. USA* **99,** 9783–9788 (2002).
16. Biswal, S. L., Raorane, D., Chaiken, A., Birecki, H. & Majumdar, A. Nanomechanical detection of DNA melting on microcantilever surfaces. *Anal. Chem.* **78,** 7104–7109 (2006).
17. Mertens, J. Label-free detection of DNA hybridization based on hydration-induced tension in nucleic acid films. *Nature Nanotech.* **3,** 301–307 (2008).
18. Backmann, N. *et al.* A label-free immunosensor array using single-chain antibody fragments. *Proc. Natl Acad. Sci. USA* **102,** 14587–14592 (2005).
19. Johansson, A., Blagoi, G. & Boisen, A. Polymeric cantilever-based biosensors with integrated readout. *Appl. Phys. Lett.* **89,** 173505 (2006).
20. Braun, T. *et al.* Conformational change of bacteriorhodopsin quantitatively monitored by microcantilever sensors. *Biophys. J.* **90,** 2970–2977 (2006).
21. Zhang, J. *et al.* Rapid and label-free nanomechanical detection of biomarker transcripts in human RNA. *Nature Nanotech.* **1,** 214–220 (2006).
22. Lang, H. P., Hegner, M. & Gerber, Ch. Cantilever array sensors. *Mater. Today* **8,** 30–36 (April, 2005).
23. Yang, M., Yau, H. C. M. & Chan, H. L. Adsorption kinetics and ligand-binding properties of thiol-modified double-stranded DNA on a gold surface. *Langmuir* **14,** 6121–6129 (1998).
24. Nelson, B. P., Grimsrud, T. E., Liles, M. R., Goodman, R. M. & Corn, R. M. Surface plasmon resonance imaging measurements of DNA and RNA hybridization adsorption onto DNA microarrays. *Anal. Chem.* **73,** 1–7 (2001).
25. Breslauer, K. J., Frank, R., Blocker, H. & Marky, L. A. Predicting DNA duplex stability from the base sequence. *Proc. Natl Acad. Sci. USA* **83,** 3746–3750 (1986).
26. Barone, F., Cellai, L., Matzeu, M., Mazzei, F. & Pedone, F. DNA, RNA and hybrid RNA–DNA oligomers of identical sequence: structural and dynamic differences. *Biophys. Chem.* **86,** 37–47 (2000).
27. Stuart, D. & Sellers, W. R. Linking somatic genetic alterations in cancer to therapeutics. *Curr. Opin. Cell Biol.* **21,** 304–310 (2009).
28. Fritz, J. *et al.* Stress at the solid–liquid interface of self-assembled monolayers on gold investigated with a nanomechanical sensor. *Langmuir* **16,** 9694–9696 (2000).
29. Valsesia, A. *et al.* Network-guided analysis of genes with altered somatic copy number and gene expression reveals pathways commonly perturbed in metastatic melanoma. *PLoS ONE* **6,** e18369 (2011).
30. Rimoldi, D. *et al.* Lack of BRAF mutations in uveal melanoma. *Cancer Res.* **63,** 5712–5715 (2003).

Acknowledgements

The authors acknowledge ongoing support from M. Despont and U. Drechsler (IBM Research GmbH) in providing cantilever arrays. The authors also thank the National Center of Competence for Nanoscale Science (NCCR Nano), the Swiss Nano Institute (SNI), the NanoTera Program, the Cleven Foundation and the Swiss National Science Foundation for financial support. K. Muehlethaler is thanked for excellent technical assistance.

Author contributions

F.H., D.R. and C.G. conceived the study. F.H. and D.R. designed the experiments and interpreted the data. F.H. performed and analysed the experiments. D.R. prepared DNA/RNA samples and cell lines. H.P.L. gold-coated the cantilever arrays. F.H., D.R., H.P.L., C.G. and N.B. wrote the manuscript. All authors discussed the results and commented on the manuscript.

Additional information

Supplementary information is available in the online version of the paper. Reprints and permission information is available online at http://www.nature.com/reprints. Correspondence and requests for materials should be addressed to F.H.

Competing financial interests

The authors declare no competing financial interests.